

# MACRO-SHEAR BOND STRENGTH AND MICRO-SHEAR BOND STRENGTH OF CEROMER BONDED TO METAL ALLOY AND FIBER REINFORCED COMPOSITE

Hyung-Yoon Park<sup>1</sup>, D.D.S., M.S.D., Lee-Ra Cho<sup>1</sup>, D.D.S., M.S.D., Ph.D.,  
Kyung-Mo Cho<sup>2</sup>, D.D.S., M.S.D., Ph.D., Chan-Jin Park<sup>1</sup>, D.D.S., M.S.D., Ph.D.

<sup>1</sup>Department of Prosthodontics, <sup>2</sup>Department of Conservative Dentistry,  
College of Dentistry and Research Institute of Oral Science, Kangnung National University

**Statement of problem.** According to the fracture pattern in several reports, fractures most frequently occur in the interface between the ceromer and the substructure.

**Purpose.** The aim of this *in vitro* study was to compare the macro shear bond strength and micro-shear bond strength of a ceromer bonded to a fiber reinforced composite (FRC) as well as metal alloys.

**Material and methods.** Ten of the following substructures, type II gold alloy, Co-Cr alloy, Ni-Cr alloy, and FRC (Vectris) substructures with a 12 mm in diameter, were imbedded in acrylic resin and ground with 400, and 1,000-grit sandpaper. The metal primer and wetting agent were applied to the sandblasted bonding area of the metal specimens and the FRC specimens, respectively. The ceromer was placed onto a 6 mm diameter and 3 mm height mold in the macro-shear test and 1 mm diameter and 2 mm height mold in the micro-shear test, and then polymerized. The macro- and micro-shear bond strength were measured using a universal testing machine and a micro-shear tester, respectively. The macro- and micro-shear strength were analyzed with ANOVA and a post-hoc Scheffe adjustment ( $\alpha = .05$ ). The fracture surfaces of the crowns were then examined by scanning electron microscopy to determine the mode of failure. Chi-square test was used to identify the differences in the failure mode.

**Results.** The macro-shear strength and the micro-shear strength differed significantly with the types of substructure ( $P < .001$ ). Although the ceromer/FRC group showed the highest macro- and micro-shear strength, the micro-shear strength was not significantly different from that of the base metal alloy groups. The base metal alloy substructure groups showed the lowest mean macro-shear strength. However, the gold alloy substructure group exhibited the least micro-shear strength. The micro-shear strength was higher than the macro-shear strength excluding the gold alloy substructure group. Adhesive failure was most frequent type of fracture in the ceromer specimens bonded to the gold alloys. Cohesive failure at the ceromer layer was more common in the base metals and FRC substructures.

**Conclusion.** The Vectris substructure had higher shear strength than the other substructures. Although the shear strength of the ceromer bonded to the base metals was lower than that of the gold alloy, the micro-shear strength of the base metals were superior to that of the gold alloy.

## Key Words

Macro-shear bond strength, Micro-shear bond strength, Ceromer, Fiber-reinforced composite

The ceramic optimized polymer (ceromer)/fiber-reinforced composite (FRC) system is composed of a load bearing fiber framework and a veneering composite filled with a large number of ceramic particles.<sup>1</sup> Clinical studies on fiber-reinforced restorations have shown a relatively high success rate over a relatively short term evaluation period.<sup>2,3</sup>

One of the ceromer/FRC systems currently available is the Targis/Vectris (Ivoclar, Schaan, Liechtenstein) system that was introduced in 1996.<sup>4</sup> Targis, which is a second generation composite material, contains a silanated microhybrid inorganic filler embedded in a light polymerizing organic matrix to improve the mechanical properties.<sup>1</sup> Vectris, which is a preimpregnated glass fiber with 3 different shapes, is formed by vacuum/pressure adaptation.<sup>4</sup> This system is purported to provide metal-free restorations that have similar mechanical properties to dentin, excellent aesthetics, ease of fabrication and repair, and are biocompatible.<sup>1</sup>

Combining the use of a ceromer over a metal substructure also could be available. The method of ceromer bonding to the metal alloy was used mainly to mask the metals such as those in the double crown removable partial dentures and resin bonded fixed partial dentures. When a ceromer material is used to veneer a metal alloy, frequent re-fabrication is needed as a result of fracture. Both chemical and mechanical bonding techniques have been proposed to avoid a detachment of the ceromer materials from the alloys.<sup>5,6</sup> The former is comprised of functional monomers that are contained in resin or surface conditioning materials, whereas the latter includes retentive beads and air-abrasion with aluminium oxide.<sup>7</sup>

Restoration failure when using a ceromer/FRC has been reported by several authors.<sup>8</sup> In their study that followed up 41 posterior FRC inlay fixed partial denture (FPD) for 4 years, Monaco et al.<sup>9</sup>

reported the causes of restoration failure to be veneer fracture in 5%, color match failure in 29%, surface texture failure in 12%, and discoloration in 4%. Behr et al.<sup>10</sup> reported that veneer fracture occurred in 36% of FPDs after using 38 inlay FPDs and single molar crowns for 4.4 years. Considering the fact that the veneer fracture is a failure in the interface of a veneer material and substructure, it appeared that there is a problem with the bonding strength of the ceromer and FRC despite having a similar matrix composition each other.

A variety of tests for measuring the bond strength of veneer-substructure systems have been advocated. The bonding strength between two substances is measured using indices such as the tensile bond strength, the shear bonding strength, and the flexural bond strength.<sup>11</sup> The tensile bond strength is gained by measuring the tension in a body when it is subjected to two set of forces that are directly away from each other. Shear is the result of two sets of forces directed parallel to each other. The flexural bond strength is measured with a 3-point bending or 4 point-bending test using a brittle material. None can be regarded as providing an exact measure of the adhesion of the veneer to substructure. Shear bond testing has been widely used mainly because of its simplicity such as the ease of specimen preparation, simple test protocol and the ability to rank different products according to bond strength values.<sup>12,13</sup>

There are several factors affecting the bond strength between the veneer-substructure, such as the type of the substructure, the treatment method for the substructure, the type of the veneer material, the bonding technique, and the experimental conditions.<sup>5-10</sup> Many studies on the bond strength between metal and resin have been conducted. Chang et al.<sup>14</sup> reported that the tensile bond strength between the resin and Au-Pa alloy was 13 MPa. It is known that the shear

bond strength between the resin and Ni-Cr ranges from 10 to 18 Mpa.<sup>15-17</sup> Kim et al.<sup>18</sup> reported that the shear bond strengths between various resins and Co-Cr alloy range from 10 to 20 MPa, and Pesun et al.<sup>19</sup> reported them to be 11-17 MPa. There have been few reports on the shear strength of the ceromer bonded to different substructure. Almilhatti et al.<sup>7</sup> reported that the shear bond strength between Targis and Ni-Cr was 12 MPa. Yoon et al.<sup>20</sup> stated that the shear bond strength was 14 to 20 MPa, whereas the shear bond strength of the metal alloys differed according to the combination between the metal alloy and the ceromer.

However, there is some question as to its validity since previous conventional shear bond strength tests have several problems. The conventional shear bond test uses mixed mode loading, in which the shear and tensile forces are induced during the test. Furthermore, there is a problem with stress concentrations at the point of loading.<sup>21</sup> Tantbirojn et al.<sup>22</sup> addressed the incapability of the discriminating the bonding state in the conventional shear test. Several alternative tests aimed at overcoming the difficulties inherent in the conventional shear test have been suggested. McDonough et al.<sup>21</sup> proposed the use of the micro-bond test to assess the strength and durability of the interface. They suggested the micro-shear bond test could be a useful tool to understand the complex interactions that occur at the interface between the two materials.

Therefore, the main purpose of this experiment was to compare the macro-shear bond strengths and the micro-shear bond strengths of the ceromer bonded to the metal alloy surfaces and FRC surface.

## MATERIAL AND METHODS

Cylinders of the dental composite resin were bonded to a prepared substructure surface, the macro-shear and micro-shear was tested at a

specified rate, and the interfacial bond strengths were calculated.

### Macro-shear bond testing

Twenty button shaped wax patterns (Baseplate wax, Kim's International, Seoul, Korea) were formed in an acryl mold, 12mm in diameter and 3mm in length. All the wax specimens were invested under vacuum with a complete investment (Micro-Fine 1700, Talladium, Valencia, USA). After burnout at the temperatures specified by the manufacturer, the specimens were centrifugally cast in metal alloys according to the manufacturer's instructions; Co-Cr alloy (Biosil, Degussa Dental, Postfach, Germany), Ni-Cr alloy (Rexillum III, Pentron, Wallingford, USA) and type II gold alloy (A48; AlphaDent, Seoul, Korea). The alloy was melted with a gas-oxygen multi-orifice torch. The remaining parts of the investment were removed by sandblasting with 110 $\mu$ m aluminum oxide. The disk area of the test surface of each specimen was calculated using the mean of three measurements made at separate locations with an accuracy of 0.01mm.

Ten FRC specimens were fabricated using an acryl mold with the same dimensions. Layers of the Vectris Pontic were placed into the acryl mold and light-polymerized for 10 minutes under a vacuum/pressure (1.5 psi) (Vectris VS1 unit, Ivoclar, Schaan, Liechtenstein; contains two 65W halogen bulbs). The polymerized fiber framework was removed from the acryl mold. The framework was then trimmed to ensure that each group had the same dimension as the metal disc. Metal specimens and FRC specimens were embedded in a 20  $\times$  20  $\times$  5 mm autopolymerizing acrylic resin (Orthojet, Lang dental Mfg. Wheeling, USA).

After polymerization, metal surfaces were ground on an Automet grinder/polisher (Buehler Ltd, Evanston, USA). The initial rough grinding was accomplished with 400 grit sandpaper, fol-

lowed by polishing with 1,000 grit sandpaper. The metal and FRC surfaces were air abraded for 5 seconds with 50  $\mu\text{m}$  aluminum oxide, steam cleaned for 5 seconds, washed under running tap water, and then dried with oil-free compressed air until complete dry.

The metal primer (Targis link; Ivoclar, Schaan, Liechtenstein) was applied to the pretreated bonding area of the metal specimens, and dried for 1 minute as recommended by the manufacturer. The FRC specimens received a coating of a wetting agent (Vectris wetting agent; Ivoclar, Schaan, Liechtenstein) with a single brush application, which was allowed to dry for 1 minute.

Thereafter, the ceromer was applied to a 6 mm diameter and 3 mm height mold positioned on the bonding surface of the substructure. Two layers of the 1.5 mm ceromer were incrementally pre-polymerized using a halogen light source (180  $\text{mW}/\text{cm}^2$  at a 10 mm distance) (Targis Quick; Ivoclar, Schaan, Liechtenstein) for 10 seconds. The specimens were post-polymerized in a Targis Power Oven (Ivoclar, Schaan, Liechtenstein) using Program 1 at 90°C for 25 minutes. After polymerizing the ceromer, the acryl mold was carefully removed. The specimens were then stored in a dark room at 25°C for 24h until they were tested.

The macro-shear bond strength tests were performed with a universal testing machine (Zwick 010; Ulm, Germany) with a pushing device used at a crosshead speed of 1.0 mm/min until fracture. The shear bond strengths were calculated according to the formula:  $B = F/S$ . ( $B$ : shear bond strength (MPa),  $F$ : load at fracture (N), and  $S$ : bonded surface area ( $\text{mm}^2$ ).

### Micro-shear bond testing

Three types of substructures (10 specimens for each), 6mm in diameter and 3mm in length, were fabricated and pre-treated with the same method described previously. Subsequently, a thin layer of Targis was light polymerized. Targis

was subsequently filled into an iris cut from microbore Tygon tubing (TYG-030, Small Parts Inc., Miami Lakes, USA) with an internal diameter approximately 1.0mm and a height of 2.0mm. The iris was held firmly on the surface using a double-sided tape to prevent the ceromer from seeping away from the defined area at the base. After this step, the ceromer was polymerized. Thereafter, the Tygon tubing was removed. All samples were checked for bonding defects using an optical microscope ( $\times 30$ ). The samples that showed an apparent interfacial gap formation, bubble inclusion, or other obvious defects were excluded from this study.

The ceromer-substructure bonds were subsequently broken by the micro-shear testing. The test device was suspended on a rod that was connected to a load cell (EZ test; Shimadzu Co., Japan). The 0.02 mm ligature wire (Tomy International, Inc., Tokyo, Japan) of the micro-shear apparatus was hooked around the cylinder of the ceromer to be tested (Fig. 1). The wire tension was controlled so as not to introduce pulling forces before the micro-shear test. During the test, the ligature wire of the ceromer was pulled from the substructures at a rate of 1.0mm/min. The change in the load as a function of time was recorded on a

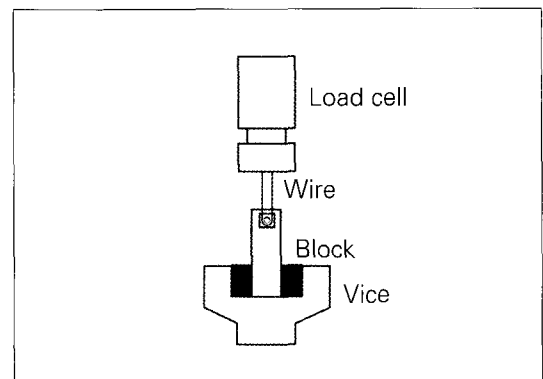


Fig. 1. Schematic diagrams of the micro-shear strength.

computer and the shear strength was calculated from the equation,  $\tau = F / (\phi R^2)$ , where  $\tau$  was the interfacial shear strength,  $F$  was the load at failure and  $R$  was the radius of the ceromer cylinder.

### Fracture mode

After testing, all the specimens were examined using a stereomicroscope (SZH-ILLB, Olympus Optical Co., Tokyo, Japan) at x 10 magnification to analyze the pattern of failure. The fracture modes were divided into the adhesive fracture and cohesive fracture groups. The former was a failure in the interface between the veneer material (Targis) and the substructures. The latter was classified as a fracture in the veneer material or in the substructures. Subsequently, the fracture surface of the specimens was examined by scanning electron microscopy (SEM, LEO 420; LEO LTD, Cambridge, UK) to investigate the surface morphology at the failure site.

### Statistical analysis

The macro- and micro-shear strengths were analyzed using one-way ANOVA to determine if

significant differences existed at the 95% confidence level. When the differences were significant, a multiple comparison test was performed using the Scheffe's method. Statistical analyses within the groups with regard to the test methods (macro- and micro- shear strength) were made using Student's *t*-test. The results of the fracture patterns of each group were analyzed with nonparametric chi-square test.

## RESULTS

The macro-shear strength differed significantly with the types of substructure ( $P < .001$ , Table I). The macro-shear strength of the Targis/Vectris group (22 Mpa) was significantly higher than that of any other group ( $P < .001$ ) (Table II). The base metal substructure groups showed the lowest mean shear strength regardless of the type of alloy.

The micro-shear strength of the substructures also differed significantly ( $P < .001$ , Table III). Although the Targis/Vectris groups showed the highest micro-shear strength (25 Mpa), it was not sig-

**Table I.** Analysis of variance for the macro-shear strength.

	Sum of squares	Df	Mean Square	F	Sig.
Between Groups	1159.742	3	386.581	16.012	.000
Within Groups	869.181	36	24.144		
Total	2028.923	39			

**Table II.** Macro-shear strength (MPa) of the Targis/ Substructure.

Bond type	Mean shear strength $\pm$ SD
Targis/gold alloy	17.4 $\pm$ 1.5
Targis/Cr-Co alloy	13.3 $\pm$ 1.9
Targis/Ni-Cr alloy	13.0 $\pm$ 2.8
Targis/FRC	22.2 $\pm$ 5.7

Shear strength joined by vertical lines are significantly different from each other ( $P < .05$ )

nificantly different from the Targis/base metal alloys ( $P=.326$ , Table IV). The gold substructure group (17.4 Mpa) exhibited the lowest micro-shear strength. The micro-shear strength was higher than the macro-shear strength with the exception the gold substructure group. In particular, the micro-shear strength of the Cr-Co substructure group was significantly higher than the macro-shear strength ( $P=.000$ ).

The results of the failure mode are shown in Table V. Nonparametric chi square test for both the macro-shear and micro-shear strength showed that there were significant differences in the failure patterns among the 4 groups. Adhesive failure was most frequent in the ceromer specimens

bonded to the gold alloys. Three and none of the ten ceromers bonded to the FRC exhibited adhesive failure in the macro-shear test and the micro-shear test, respectively.

Figure 2 shows the SEM images of fractured interface between the veneer and the substructures. Because all images were taken at the outer boundary of the ceromer, the left side indicated the substructure and the right side indicated the remnant of the ceromer. The alloy substructures exhibited a crystalline structure. After comparing the gold alloys substructure, the Ni-Cr alloy and Cr-Co alloy substructure showed a mainly cohesive failure pattern.

**Table III.** Analysis of the variance for the micro-shear strength.

	Sum of squares	Df	Mean Square	F	Sig.
Between Groups	907.657	3	302.552	6.783	.001
Within Groups	1605.865	36	44.607		
Total	2513.521	39			

**Table IV.** Micro-shear strength (MPa) of the Targis/Substructure.

Bond type	Mean micro-strength $\pm$ SD
Targis/gold alloy	16.3 $\pm$ 3.9
Targis/Co-Cr alloy	20.2 $\pm$ 5.8
Targis/Ni-Cr alloy	20.9 $\pm$ 4.6
Targis/FRC	25.2 $\pm$ 4.4

Micro-shear strength joined by vertical lines are significantly different from each other ( $P<.05$ )

**Table V.** Fracture mode after the loading test.

Bond type	Macro-shear test		Micro-shear test	
	Adhesive failure (%)	P-value	Adhesive failure (%)	P-value
Targis/gold alloy	70	$P = .010$	70	$P = .002$
Targis/Co-Cr alloy	30	$\chi^2 = 11.282$	30	$\chi^2 = 14.420$
Targis/Ni-Cr alloy	0	$DF = 3$	10	$DF = 3$
Targis/FRC	30		0	

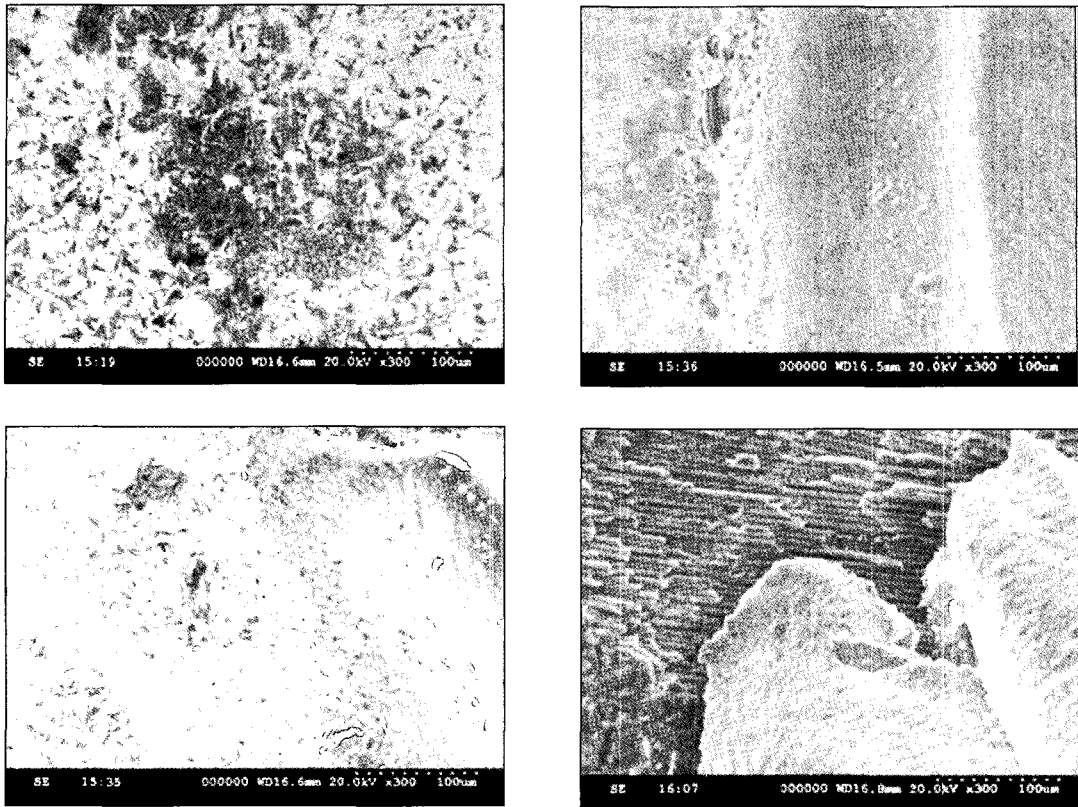


Fig. 2. Typical scanning electron microscopic views of the ceromer bonded to four substrates. (A) Adhesive failure in the interface between the ceromer and the gold alloys. (B) Cohesive failure at the ceromer bonded to the Ni-Cr alloys. (C) Cohesive failure at the ceromer bonded to the Co-Cr alloys. (D) Cohesive failure at the ceromer bonded to the FRC substructure. (Original magnification  $\times 300$ ).

## DISCUSSION

The macro-shear bond strength was the highest in Vectris, followed by the gold alloy and base metal alloy. Otherwise, the micro-shear bond strength was higher in the base metal alloy compared to the gold alloy. Adhesive failure occurred in 70% of all gold samples when conducting the macro-shear bond test and the micro-shear bond test. The frequency of adhesive failure in the Ni-Cr alloy or Vectris was relatively low. Considering that the adhesive failure is an indirect index of the shear bond strength between the veneer and substructure, frequent adhesive failure suggests low bond strength. These results overall suggest that

the micro-shear bond test is more accurate in showing the bond strength of the interface. Furthermore, the micro-shear strength was higher than the macro-shear strength in all substrates except for the gold alloy. It appeared that these results were brought about from the fact that the tensile force would participate to accelerate failure in the later loading time of the macro-shear test. Therefore, the bond strength per area would be higher in the micro-shear test than the macro-shear test.

The macro-shear bond strength was lower in the base metal alloy (13 MPa) compared to the gold alloy (17 MPa) in this study, which is similar to that reported by Laufer et al.<sup>23</sup> However, Yoon et al.<sup>20</sup>

reported that the shear strength of the Ni-Cr alloy was higher than that of the gold alloy. Rubo et al.<sup>24</sup> also reported that the bond strength was the highest in the Ni-Cr alloy, followed by the Ag-Pd alloy and the gold alloy. These results are consistent with the rank of the micro-shear strength found in this study. Overall, although the bond strength of the veneer and the substructures differed according to the testing conditions, the test method would also affect the data according to the results of this study.

Both the Vectris and Targis contain Bis-GMA and decandiol in the matrix.<sup>1</sup> Therefore, it was expected that they would have higher bond strengths than the other substructures. However, no statistically significant difference was observed in the micro-shear bond strength compared to that of the base metal alloy, which suggested that the veneer failure was due to low bond strength. In addition, interface failure in the Targis/Vectris crown and Targis cleavage from Vectris in a previous study<sup>25,26</sup> were probably due to the lower bond strength than was expected.

In this study, all the substructures were sandblasted to give the same surface treatment. This treatment could work to lower the bond strength by removing the oxygen inhibition layer, a layer with several microns that develops from oxygen in the air binding with the monomer on the composite resin surface. This layer does not completely undergo polymerization even with light polymerizing. Therefore, this layer becomes the layer where additional composite resin could chemically adhere.<sup>27</sup> The removal of this layer by sandblasting could be a factor in lowering the bonding strength of the Targis/Vectris.

Moreover, a metallic oxide would form a thin and dense layer in noble metal alloys so that the bond strength would deviate slightly and have a high reliability. On the other hand, in the Cr alloy, Cr has a high oxidative power, which means that a thick oxide layer usually results. It

was reported that the bond strength would decrease as the thickness of the metallic oxide layer would increase.<sup>20</sup> The bonding area of the sample used in the micro-shear test was small in this study. Therefore, it appears that the micro-shear strength in the base metal was higher compared to the macro-shear strength, because the effect of the thick oxide layer decreased.

The bonding technique also affected the study result. In the macro-shear test, one layer of Targis, which was approximately 1.5 mm was firstly light polymerized and the other 1.5 mm was then polymerized in order to build-up a 3 mm thickness. On the other hand, in the micro-shear test, the sample thickness (2 mm) was small so that one thin Targis layer was polymerized and the rest was built-up. In other words, the bond strength of the interface was affected since polymerization contraction of the thin Targis layer was less than that of the thick macro-shear bond strength (1.5 mm) for the micro-shear bond strength.

It is also known that the type of veneer material would also affect the bond strength resulting in different bond strengths according to the combination of ceromer/metal alloy.<sup>6,13-19</sup> However, in this study, only one veneer material was used to obtain more conclusive results.

The limitation of this study was the fact that a static test was performed in a dry environment. Water would be constantly present in the actual oral environment, which would undergo repeated temperature and pH changes. According to most studies on the bond strength, the actual bond strength would be lower than expected since the bond strength would decrease further with thermocycling or artificial aging.<sup>28</sup>

Despite this limitation, the macro-shear bond strength and micro-shear bond strength of various substructures and interfaces were tested and compared. The results of this study showed that the micro-shear bond strength would be a better method for reflecting the bond strengths of the two



materials. Furthermore, the bond strength of the Targis bonded to the gold alloy was too weak, which means that new methods will be needed to improve the strength. In addition, the bond strength of the Targis/Vectris having the same matrix was not that high compared to the theoretical bond strength. Therefore, these results might explain the mechanism of various types of failure that occur in actual clinical situations.

## CONCLUSION

Based on the conditions in this in vitro study, it was concluded that the type of substructure has an influence on the shear strength of ceromer/substructure. The Vectris substructure had higher shear strength than the other substructures. The shear strength was different from the micro-shear strength in the same veneer/substructure group. Although the shear strength of the ceromer bonded to the base metals was lower than the gold alloy, the micro-shear strength of the base metals was superior to the gold alloy. Cohesive failure in the ceromer layer was more frequent in the FRC substructure while adhesive failure was dominant in the alloy substructures.

## REFERENCES

1. Touati B, Aidan N. Second generation laboratory composite resin for indirect restorations. *J Esthet Dent* 1997;9:108-18.
2. Göhring TN, Mörmann WH, Lutz F. Clinical and scanning electron microscopic evaluation of fiber reinforced inlay fixed partial dentures: Preliminary results after one year. *J Prosthet Dent* 1999;82: 662-8.
3. Altieri JV, Burstone CJ, Goldberg AJ, Patel AP. Longitudinal clinical evaluation of fiber-reinforced composite fixed partial dentures: a pilot study. *J Prosthet Dent* 1994;71:16-22.
4. Krejci I, Boretti R, Lutz F, Giezendanner P. Adhesive crowns and fixed partial dentures of optimized composite resin with glass fiber-bonded framework. *Quint Dent Tech* 1999;22:107-27.
5. Choi NJ, Vang MS. The effects of metal surface treatment on bond strength between resin and metal interface of resin veneered crown. *J Korean Acad Prosthodont* 1994;34:471-83.
6. Martin J, LeBeau S. The best of both worlds: combining metal and ceromer for clinical success. *Dent Today* 2000;19:88-9.
7. Almilhatti HJ, Giampaolo ET, Vergani CE, Machado AL, Pavarina AC. Shear bond strength of aesthetic materials bonded to Ni-Cr alloy. *J Dent* 2003;31:205-11.
8. Freilich MA, Meiers JC, Duncan JP, Eckrote KA, Goldberg AJ. Clinical evaluation of fiber-reinforced fixed bridges. *J Am Dent Assoc* 2002;133: 1524-34.
9. Monaco C, Ferrari M, Miceli GP, Scotti R. Clinical evaluation of fiber-reinforced composite inlay FPDs. *Int J Prosthodont* 2003;16:319-325.
10. Behr M, Rosentritt M, Handel G. Fiber-reinforced composite crowns and FPDs: a clinical report. *Int J Prosthodont* 2003;16:239-43.
11. Cesar PF, Meyer Faara PM, Miwa Caldart R, Gastaldoni Jaeger R, da Cunha Ribeiro F. Tensile bond strength of composite repairs on artglass using different surface treatments. *Am J Dent* 2001;14:373-7.
12. Craig RG. . Powers J M. Restorative dental materials. 11th ed. St. Louis: CV Mosby 2002 54-71.
13. Nakamura T, Waki T, Kinuta S, Tanaka H. Strength and elastic modulus of fiber-reinforced composite used for fabrication FPDs. *Int J Prosthodont* 2003;16:549-53.
14. Chang JC, Koh SH, Powers JM, Duong JH. Tensile bond strength of composite to gold-palladium alloy after thermal cycling. *J Prosthet Dent* 2002;87:271-6.
15. Rothfuss LG, Hokett SD, Hondrum SO, Elrod CW. Resin to metal bond strength using two commercial systems. *J Prosthet Dent* 1998;79:270-2.
16. Czerw RJ, Wakefield CW, Robbins JW, Fulkerson MS. Shear bond strength of composite resin to microetched metal with five newer-generation bonding agent. *Oper Dent* 1995;20:58-62.
17. Smith RM, Barrett MG, Gardner WA, Marshall T, McLean MJ, McMichael DW, Yerbury PJ, Rawls HR. Effect of environmental stress and surface treatment on resin-to-metal bonding. *Am J Dent* 1993;6: 111-5.
18. Kim JY, Pfeiffer P, Niedermeier W. Effect of laboratory procedures and thermocycling on the shear bond strength of resin metal bonding systems. *J Prosthet Dent* 2003;90:184-9.
19. Pesun S, Mazurat RD. Bond strength of acrylic resin to cobalt-chromium alloy treated with the Silicoater MD and Kevloc systems. *J Can Dent Assoc* 1998; 64:798-802.
20. Yoon DJ, Shin SW, Lim HN, Suh KW. A study of the bond strength of reinforced indirect composite resins to dental alloys. *J Korean Acad Prosthodont* 1999;37:620-39.
21. McDonough WG, Antonucci JM, He J, Shimada Y, Chiang MY, Schumacher GE, Schultheisz CR. A microshear test to measure bond strengths of dentin-

- polymer interfaces. *Biomaterials* 2002;23:3603-8.
22. Tantbirojn D, Cheng YS, Versluis A, Hodges JS, Douglas WH. Nominal shear or fracture mechanics in the assessment of composite-dentin adhesion? *J Dent Res* 2000;79:41-48.
  23. Laufer B, Nicholls J, Townsend J. SiO<sub>x</sub>-C coating: A composit-to-metal bonding mechanism. *J Prothet Dent* 1988;60:320-7.
  24. Rubo JH, Pegoraro LF, Ferreira PM. A comparison of tensile bond strengths of resin-retained prostheses made using five alloys. *Int J Prosthodont* 1996;9:277-81.
  25. Cho L, Song H, Koak J, Heo S. Marginal accuracy and fracture strength of ceromer/fiber-reinforced composite crowns: effect of variations in preparation design. *J Prosthet Dent* 2002;88:388-95.
  26. Song HY, Yi YJ, Cho LR, Park DY. Effects of two preparation designs and pontic distance on bending and fracture strength of fiber-reinforced composite inlay fixed partial dentures. *J Prosthet Dent* 2003;90:347-53.
  27. Rueggeberg FA, Margeson DH. The effect of oxygen inhibition on an unfilled/filled composite system. *J Dent Res* 1990;69:1652-8.
  28. Lastumaki TM, Kallio TT, Vallittu PK. The bond strength of light curing composite resin to finally polymerized and aged glass fiber-reinforced composite substrate. *Biomaterials* 2002;23:4533-9.

*Reprint request to:*

CHAN-JIN PARK  
DEPT. OF PROSTHODONTICS, COLLEGE OF DENTISTRY,  
KANGNEUNG NATIONAL UNIVERSITY,  
120 GANGNEUNG DAEHANGNO, GANGNEUNG, 210-702, KOREA  
doctorcj@kangnung.ac.kr